

Thermal Effect on Void Formation of Waxy Crude Oil Using Electrical Capacitance Tomography

Areeba Shafquet^{a*}, Idris Ismail^a, Azuraïen Jaafar^b

^aElectrical and Electronic Engineering Department, Universiti Teknologi PETRONAS, Bandar Seri Iskandar 31750, Tronoh, Perak Darul Ridzuan, Malaysia

^bMechanical Engineering Department, Universiti Teknologi PETRONAS, Bandar Seri Iskandar 31750, Tronoh, Perak Darul Ridzuan, Malaysia

*Corresponding author: engr.areeba@gmail.com

Article history

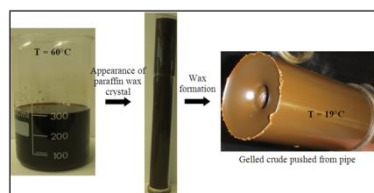
Received :21 February 2013

Received in revised form :

6 June 2013

Accepted :15 June 2013

Graphical abstract



Abstract

Waxy crude oils are commonly found in many parts of the world and represent a huge amount of the global oil reserves. Precipitation of paraffin waxes during various phases creates many problems in the oil industry. Therefore, waxy crude oils create many flow assurance issues essentially linked to them and understanding of the effect of relevant factors and phenomena are of great practical importance. In process industries, the measurement of void fraction is considerably important for sustainable operations and the erroneous calculation could be the cause of many industrial accidents. The customary approach separates the two-phases first and then measures the mixture as individual components. These methods are not favorable as they may result in the disruption of incessant industrial processes. Due to these limitations, this study is aimed to analyze the gel formation behavior of a waxy crude oil under static and dynamic cooling using non-invasive/non-intrusive experimental technique; i.e. Electrical Capacitance Tomography (ECT). This paper describes a fabrication of dual-plane ECT sensor for testing of waxy crude oil at different temperature conditions. ECT images and raw data measurements have been obtained from the two planes are then normalised and then used for image reconstruction. The findings reported in this paper represent part of an ongoing investigation that may lead to develop a cross-correlation between the two planes. The outcome of the study could be used to fully understand the phenomenon of void fraction in waxy crude based on varying the temperature and also based on the design of ECT sensor.

Keywords: Capacitance measurement; electrical capacitance tomography; thermal shrinkage; void fraction; waxy crude oil

Abstrak

Minyak mentah berlilin biasanya ditemui di kebanyakan bahagian dunia dan mewakili sejumlah besar rizab minyak global. Pemendakan lilin parafin dalam pelbagai fasa pengeluaran, pemrosesan dan pengangkutan minyak mentah berlilin mewujudkan banyak masalah dalam industri minyak. Oleh itu, minyak mentah berlilin mewujudkan banyak isu-isu jaminan aliran asasnya dikaitkan dengan mereka dan memahami kesan faktor-faktor yang berkaitan dan fenomena mempunyai kepentingan praktikal yang besar. Dalam industri proses, pengukuran 'void fraction' adalah lebih penting bagi operasi yang mampan dan pengiraan yang salah ia tidak dapat dielakkan menjadi punca banyak kemalangan perindustrian. Pendekatan khusus memisahkan dua fasa pertama dan kemudian mengukur campuran sebagai komponen individu. Kaedah-kaedah ini tidak menjadi pilihan kerana ia boleh menyebabkan gangguan proses industri berterusan. Disebabkan batasan ini, kajian ini bertujuan untuk menganalisis perlakuan pembentukan gel minyak mentah berlilin di bawah penyejukan statik dan penyejukan dinamik menggunakan teknik eksperimen 'non-invasive/non-intrusive' iaitu Tomography Kemuatan Elektrik (ECT). Tesis ini menerangkan pembentukan sensor dwi-planar ECT untuk menguji minyak mentah berlilin pada keadaan suhu yang berbeza. Imej ECT dan ukuran data yang diperolehi dari kedua-dua planar ini kemudiannya pulih dan kemudiannya digunakan untuk membina semula imej. Hasil kajian ini boleh digunakan untuk memahami sepenuhnya fenomena 'void fraction' dalam minyak mentah berlilin berdasarkan perubahan suhu, tekanan dan juga rekabentuk sensor ECT.

Kata kunci: Ukuran kapasitan; tomografi kemuatan elektrik; pengecutan haba; pecahan lompong; minyak mentah berlilin

© 2013 Penerbit UTM Press. All rights reserved.

1.0 INTRODUCTION

In the oil and gas industry, about 20% of the petroleum reserves produced and pipelined are crudes containing large proportions of high molecular weight compounds, also known as Waxy Crude Oils [1]. Waxy crude oils are commonly found in many parts of the world and represent a huge amount of the global oil reserves. Precipitation of paraffin waxes during various phases of production, processing and transportation of waxy crude oils creates many problems in the oil industry. Wax deposition on cold surface causing a reduced flow and increased pressure drop [2]. Therefore, waxy crude oils create many flow assurance issues inherently linked to them and understanding of the effect of relevant factors and phenomena are of great practical importance. The transportation of these crude oils presents a significant complexity and could cause many difficulties such as clogged pipelines especially during shutdown [3, 4]. These crude oils are light or intermediate crude containing between 2 to 10% of paraffin wax [3, 5].

Waxy crude behaves typically as a Newtonian fluid at reservoir conditions (i.e. high temperatures and pressures), having a unique viscosity at any given temperature. But as the crude flows in subsea pipelines, where it is exposed to very cold environments, it starts to cool and once the temperature drops below Wax Appearance Temperature (WAT), where the wax crystals begin to precipitate out of solution and a very rapid increase in viscosity indicates the onset of non-Newtonian flow behavior [6]. The precipitation of wax components out of the oil is responsible for changes in the waxy crude oil properties including gelation of oil and an increase in viscosity [7]. In this process, the paraffin deposit gradually ages and becomes thicker and harder with time, reducing the pipe diameter, clogging the pipeline, and reducing its flow efficiency [8].

During deliberate or unexpected production shutdowns for prolonged periods of time which is usually performed for maintenance or emergency reasons, the crude oil is stationary and under this condition, the temperature within the pipeline is subjected to the external factors and drops significantly (static cooling) as in the case for subsea installations and in the arctic regions. In a production shutdown in an offshore oil platform

occurring far away from the shore, the crude oil contained in a long-pipeline laying on the sea floor is cooled under quiescent conditions because of exposure to temperatures as low as 5°C. Thus, paraffin precipitates out of the crude oil and forms a strong paraffinic gel that can eventually cause a complete pipeline plugging where the yield stress and thixotropic behavior are further exaggerated [9]. Frequently, the gel yield stress can be extremely high, exceeding the maximum allowable pressure that the pipe material can safely bear. Under these conditions, flow cannot be restarted and the entire pipeline has to be abandoned resulting in significant economic loss for the pipeline operator.

During the gel build-up, the waxy crude undergoes thermal shrinkage where gas voids subsequently appear resulting in a, supposedly, compressible structure. A study on the thermal shrinkage entitled “Novel Approaches to Waxy Crude Restart: Part 1: Thermal Shrinkage of Waxy Crude Oil and the Impact for Pipeline Restart” had come out with a result which proven that there were gas voids produced by cooling process of the crude oil in the flow line [10]. The gas voids appearance may affect the compressibility of the gelled crude since there are spaces for the gelled crude to move after some amount of pressure applied. This assumption was also confirmed by Margarone which stated that gelled crude behaves as an incompressible high viscous fluid [11]. Vinay *et al.* (2007) observed that gas voids in the range of 4–8% of the total pipe volume, according to the shutdown conditions, are not unusual. The gel formation, governed by the paraffin crystallization, is controlled by both thermal and flow mechanisms. The location and volume of gas voids embedded in the gelled crude oil can depend strongly on the cooling and flow rates in the pipe [12]. Hénaut *et al.* (1999) reported that the shrinkage results in the void spaces which can be varied in various shapes and sizes depending on the cooling rate and temperature [13]. Figure 1 shows the transformation of waxy crude oil from liquid (at temperature of 60°C) to complete wax formation (at temperature of 19°C) that has been observed in the Instrumentation and Control laboratory of Universiti Teknologi PETRONAS (UTP) during an experimental analysis.

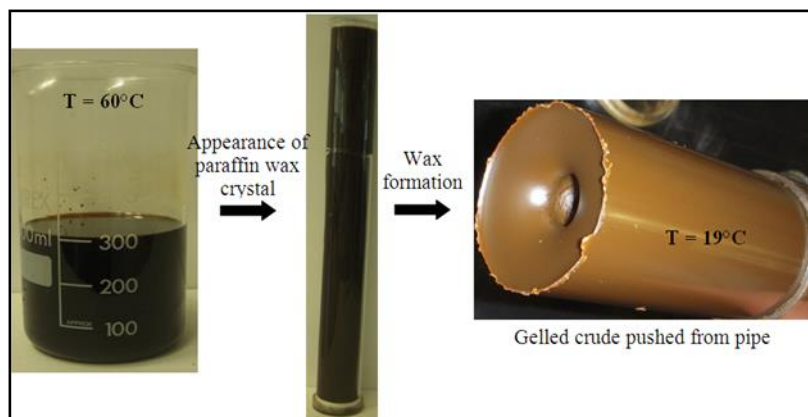


Figure 1 Appearance of gas void and transformation of crude oil into waxy crude

However, there are several remediation techniques available, such as sending divers to manually remove the pipeline blockage, mechanical pigging, and melting the deposit by heat generated via chemical reaction [14]. Mechanical pigging consists of removing the solid deposits on the pipe wall

using a scraper device. However, this operation may have complications when the gel strength is very high and the pig may get stuck in the pipeline during the cleaning process.

It is essential to take into account the multiphase's of fluid present in a crude together with the thermal shrinkage and gas

voids formed during cooling. In process industries, the measurement of void fraction is considerably important for sustainable operations. The erroneous calculation of void fraction is inevitably be the cause of many industrial accidents such as loss of coolant accidents in nuclear reactor, sweet corrosions in subsea oil and gas pipelines and an in-efficient process control of chemical plants. Due to this reason, the void fraction is considered as a critical parameter for designing pipeline system in the above process applications. In case of any accident, a large amount of expenditure is required for the installation and replacement of pipelines. It is therefore, necessary to measure and control the void fraction for achieving safety, process efficiency, energy saving and quality assurance in the process applications. So it is therefore, necessary to predict this parameter in waxy crude oil in order to understand its behavior deeply.

The present study is, therefore, undertaken with the aim of designing and fabricating a dual-plane ECT sensor for the analysis of thermal effect on void fraction in Waxy Crude Oil. The main objective of this paper is to analyze the thermal response on capacitance and pixel based void of the crude oil under static and dynamic cooling in dual-plane ECT sensor.

2.0 MATERIALS AND METHODS

2.1 Electrical Capacitance Tomography (ECT)

Electrical Capacitance Tomography (ECT) is a non-intrusive and non-invasive technique for finding out the internal fluid flow characteristics [15]. It has been developed for imaging industrial processes containing dielectric materials and based on measuring the changes in dielectric material distribution. It has also been used to achieve real time visualization of industrial processes and measure void fraction for two-phase flow. It also provides the quantitative measures of flow which is used for image and flow rate information [15]. ECT system mainly comprises three main components: (1) a capacitance sensor, (2) data acquisition system, and (3) control computer for reconstruction as shown in Figure 2.

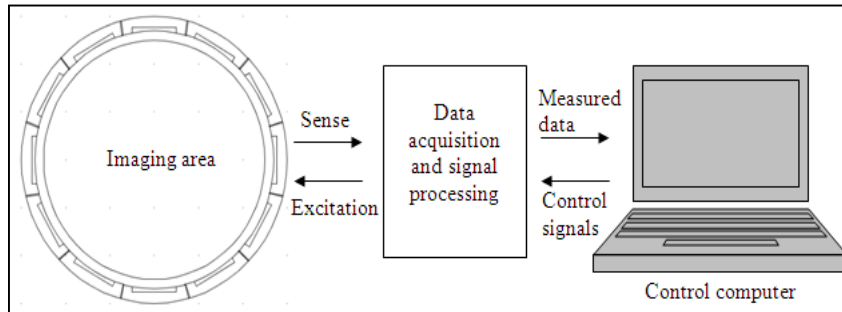


Figure 2 Basic ECT system

The ECT sensor cross-sectional model and the basic capacitance measurement principle used in ECT are shown in Figure 3. It comprises 12 copper plates which are installed on the outer periphery of the pipe. There is a radial grounding plate between two adjacent electrodes for reducing the adjacent electrodes capacitance value. It is acting as a grounded screen for shielding the entire system and also making it not to interfere

from stray fields [16, 17]. The 12 electrode system as shown in Figure 3 is numbered and excited by an electric potential in an increasing order. In tomography, the object to be imaged is surrounded by electrodes, which acts as both sources and detectors. The electrodes are excited one by one, or in pairs depending on the protocol used.

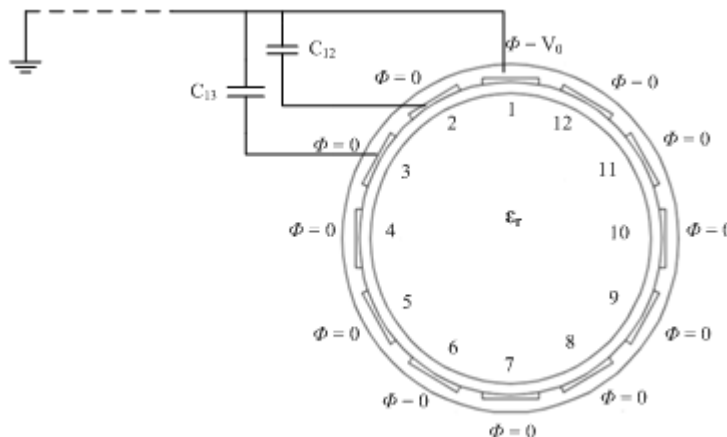


Figure 3 Schematic representation of the measurement principle of an ECT system

There are number of protocols used in ECT measurements but *Protocol 1* is the most widely used in data acquisition systems for ECT. According to this protocol, only one electrode is excited at any point in time and the remaining electrodes are kept at ground potential and function as detectors until the measurement completes the full cycle or $N-1$ electrodes [17].

During a measurement period, each electrode in an ECT sensor is energized by applying an excitation voltage signal, and the induced charge/current is detected from all other electrodes while their potential is kept at zero. For example, in the first step, to obtain a complete set of data for one image, electrode 1 is used for excitation by applying a potential and electrode 2 to 12 for detection as they connected to virtual ground terminals, so that they remain at zero potential with respect to the ground, obtaining 11 capacitance measurements and this process continues until electrode $N-1$ is excited. In this way, there will be 66 independent capacitance measurements, which are governed by the following equation [18]:

$$M = \frac{N(N-1)}{2} \quad (1)$$

where, M is independent inter-electrode capacitance measurement and N is the number of electrodes located around the circumference.

Normalisation is commonly used to calibrate an ECT system quantitatively between fixed points. It is important for ECT data due to very small capacitance values. When a mixture of two dielectric materials is imaged, an ECT system is calibrated by measuring two reference sets of inter-electrode capacitances. The sensor is first measured empty, i.e. using air to find the lower capacitance C_l having a lower permittivity limit, then it is completely filled with material having a higher permittivity limit to acquire the values for higher capacitance, C_h . All consequent measured capacitance values, C_m , are then normalised to have values C_n because when capacitance values are involved they are always normalised between '0' (when the sensor fully filled with lower permittivity material) and '1' (when the sensor fully filled with higher permittivity material) as shown in equation (2) [19].

$$C_n = \frac{C_m - C_l}{C_h - C_l} \quad (2)$$

2.2 Void Fraction Measurement (VFM)

The term *voidage*, *volume ratio* or *concentration* can be defined as the percentage of the volume of the sensor occupied by the higher permittivity material. The volume of the sensor is the product of the cross-sectional area of the sensor and the length of the measurement electrodes. The overall void of the contents of ECT sensor can be calculated using two methods [17]:

- (1) Using normalised pixel values in the reconstructed ECT image, or
- (2) The normalised capacitance measurements.

All voidage values obtained from the ECT system were based on the assumption that the voidage is 100%, when the sensor was full of the higher permittivity material and was zero when the sensor is full of lower permittivity material.

2.3 Dual Plane Sensor (DPS)

The main design parameters of an ECT sensor include the dimensions of the sensor, number of electrodes, type of electrostatic shielding, sensitivity; axial resolution and spacing between the planes (for dual-plane sensor) need to be considered carefully. Normally 12 electrodes are used, eight electrodes are more common for high sensitivity application [20]. A sensor configuration used in this study is a twin or dual plane ECT sensor. It has been designed and fabricated, with one plane at the upstream (consists of 12 electrodes) and other at the downstream (consists of 12 electrodes). The specifications are mentioned in Table 1 and the physical layout of a sensor with external shielding is shown in Figure 4.

Table 1 Specifications of dual plane ECT sensor

Parameters	Measurement
Outer diameter	60 mm
Inner diameter	54 mm
Thickness of pipe	3 mm
Number of electrodes	12 (per plane)
Number of planes	2
Length of pipe	500 mm
Length of measurement electrodes	100 mm
Width of electrodes	10 mm
End guards width	12 mm
Distance b/w end guard and measurement electrode	10 mm
Material of pipe	Acrylic
Relative Permittivity (ϵ_r)	3.0
Distance b/w two planes	54 mm to 100 mm



Figure 4 Dual plane ECT sensor with external shield

2.4 Effect of Temperature on Normalised Capacitance and Pixel based Void

The average voidage can be obtained by using the normalised interelectrode capacitance measurements. It is done by summing all the normalised capacitance values for one image and dividing these by the sum of the normalised capacitances when the sensor is filled with higher permittivity material. This can be expressed in mathematical form as follows [17];

$$VR = \frac{1}{N} \sum_{n=1}^N \left(\frac{C_n}{C_k} \right) \tag{3}$$

where, N is the total number of electrode pair measurements, C_n is the individual electrode pair normalised capacitances and C_k is the electrode pair capacitances when the sensor is full of the higher permittivity material.

The void fraction can also be calculated using the number of pixels obtained from image reconstruction using ECT [21]. In the case of calculation from image pixels, the voidage is calculated by summing the values of the individual pixels in the ECT image for the required image frame and dividing it by the sum of these pixel values when the sensor is full of higher permittivity material [17].

$$VR = \frac{1}{P} \sum_{i=1}^P \left(\frac{P_i}{P_k} \right) \tag{4}$$

where, P is the total number of pixels, P_i is the value of the i^{th} pixel and P_k is the value of the i^{th} pixel when the sensor is full of the higher permittivity material.

3.0 RESULTS AND DISCUSSION

3.1 Calibration of a Sensor

The calibration of an ECT sensor is very important and necessary step in order to ensure the reliability of capturing the images accurately. When a mixture of two dielectric materials has to be imaged then ECT systems are preferred to be calibrated. ECT sensors are calibrated by measuring two reference sets of inter-electrode capacitances; one is for a lower permittivity followed by a higher permittivity material. For this study, a sensor was calibrated using two different materials i.e., air and deionized water. They have different dielectric properties, particularly the permittivity value. So for this case, the sensor was first measured empty i.e. using air having the permittivity equals to one, and then it was completely filled with deionized water having the higher permittivity equals to 80.

The calibration has been done using the dual-plane ECT sensor whose results were analyzed on the software. As a first step, the sensor has been filled with air (empty) to perform the low calibration. Then it was filled with deionised water having higher permittivity than crude oil to perform the high calibration. The calibration data retrieved from the acquisition system was based on average measurements and has been converted to the following tomogram images (Figure 5). The low calibration data indicates a blue tomogram and high calibration data indicates a red tomogram image. The tomogram images of the calibration are based on the normalised values from 0 to 1. The color-scale for ECT is used to display the variation in permittivity between 0 to 1, indicating 0 as low permittivity and 1 as high permittivity.

Figure 6 also illustrates the voltage line graph in which air (low) has high voltage values while deionised water (high) indicates the low voltage values. This is expected because deionised water (high calibration) has permittivity of 80 while air (low calibration) has permittivity of around 1. This line graph also shows a good symmetrical curve between air and water measurements, indicating a measurement span and the sensitivity

of the sensor. In the following graph, X-axis indicates the number of electrode pairs and Y-axis indicates the voltage value.

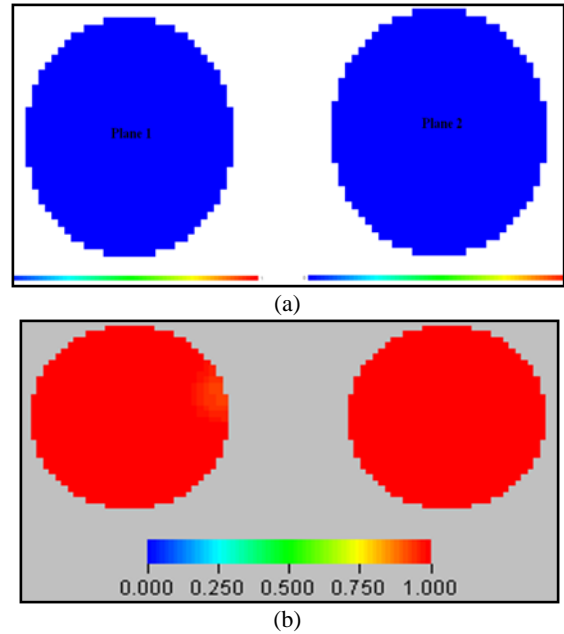


Figure 5 Calibrated tomogram image of dual-plane ECT sensor: (a) low (air) and (b) high (deionised water)

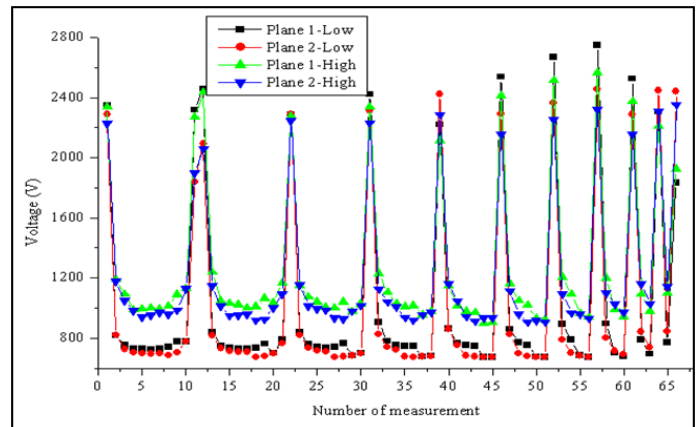


Figure 6 Low vs. high calibration line graph for dual-plane ECT sensor

3.2 Online Measurement of Crude Oil using Dual-Plane Sensor

The sample of crude oil investigated for this study is from a Malay Basin field in Malaysia. The wax content is 18wt% and Wax Appearance Temperature (WAT) is 37°C, since the WAT is high, this shows that it is heavy oil or black oil which is very thick and has high viscosity. This crude oil is also known to gel up at lower temperatures which would cause problems of transporting the crude oil to shore.

The crude oil has the tendency to separate into heavy part and light part due to density difference if it is stored for a long period of time. That is why before commencing the experiment, the crude oil is prepared to allow normal mixing process. The crude is heated up to 60°C for two hours of agitation process. This is to make sure that the crude becomes homogeneous and has good mixing between heavy part and light part (at 60°C, the

crude will behave as Newtonian fluid). The crude oil needs to be stirred as to maintain fine homogeneity characteristic during heating. When it reaches around 60°C, it has been poured into ECT sensor for online measurement, based on temperature change.

The experiments were carried out in an Instrumentation and Control laboratory of UTP at a temperature of $20 \pm 2^\circ\text{C}$. The online measurement for the statically cooled waxy crude was measured from 60°C to 21°C and subsequent measurements were observed when the dynamically cooled waxy crude oil temperature dropped until 5°C using an ice bath. The temperature of crude oil has been varied from 60°C to 5°C thus affecting the properties and characteristics of waxy cooled crude oil in a dual-plane sensor. Data for raw capacitance was collected for every 5°C change in temperature (Figure 7). The distribution of raw capacitance is well within the acceptable range of low and high calibration data. The trend of graph for raw capacitance followed by all the measurements is also symmetrical.

Based on the raw capacitance values obtained, the measurement shows that as the surrounding temperature varies there will be some significant correlation towards the sensitivity

of the electrodes in ECT sensor. As the temperature decreases gradually from 60°C to 5°C, the capacitance measurement seem to keep very close to each other however, there are constant trending showed in both planes (Figure 7).

After a good calibration data has been achieved then the sensor was completely filled with the crude oil starting from the temperature of 60°C until it take measurement at 5°C. Figure 8 shows the typical tomogram images at different temperatures. The ECT images were reconstructed from the capacitance signals using Linear Back Projection (LBP) algorithm from the upstream and downstream sensor. The LBP method offered fast processing time in comparison with other algorithms; however, it did produce qualitative, rather than quantitative, images. The images represent the cross-sectional phase distribution inside the sensor. The color scale of ECT represents the variation in permittivity from 0 to 1 i.e. blue to red (low to high). It shows a region of low concentration in the centre of the pipe and a region of high concentration close to the wall of the sensor. Although the data obtained from the tomogram images is quiet limited but this initial finding can lead towards another hypothesis for further research.

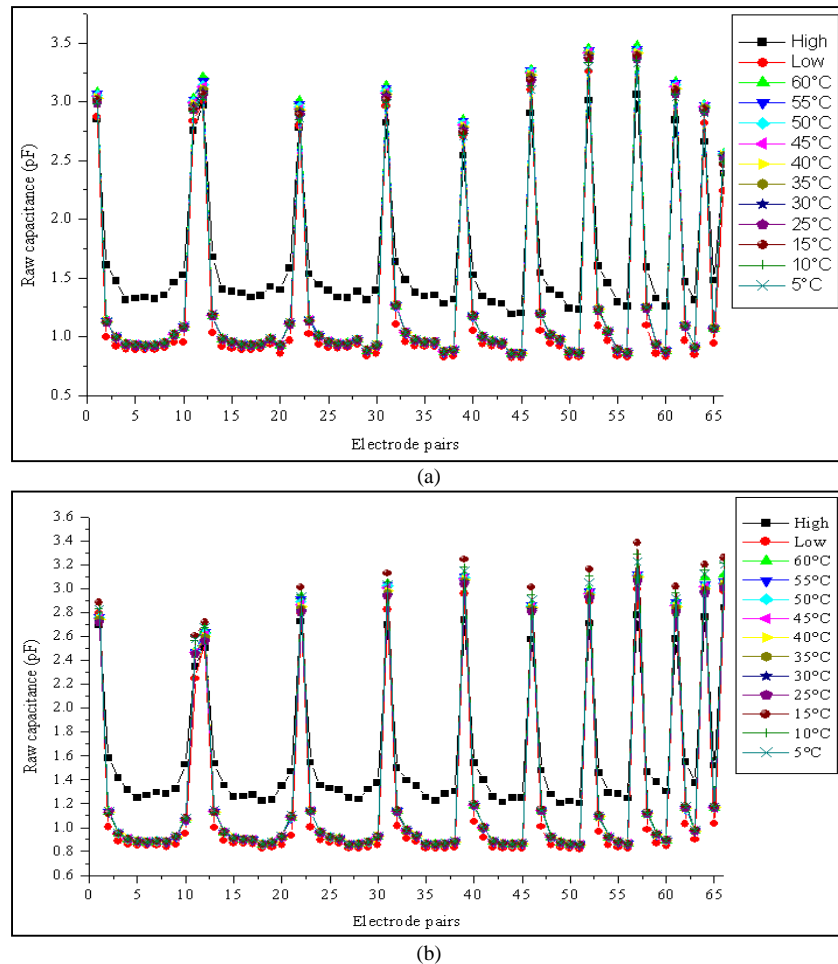


Figure 7 Raw capacitance obtained at different temperatures: (a) Plane 1, and (b) Plane 2

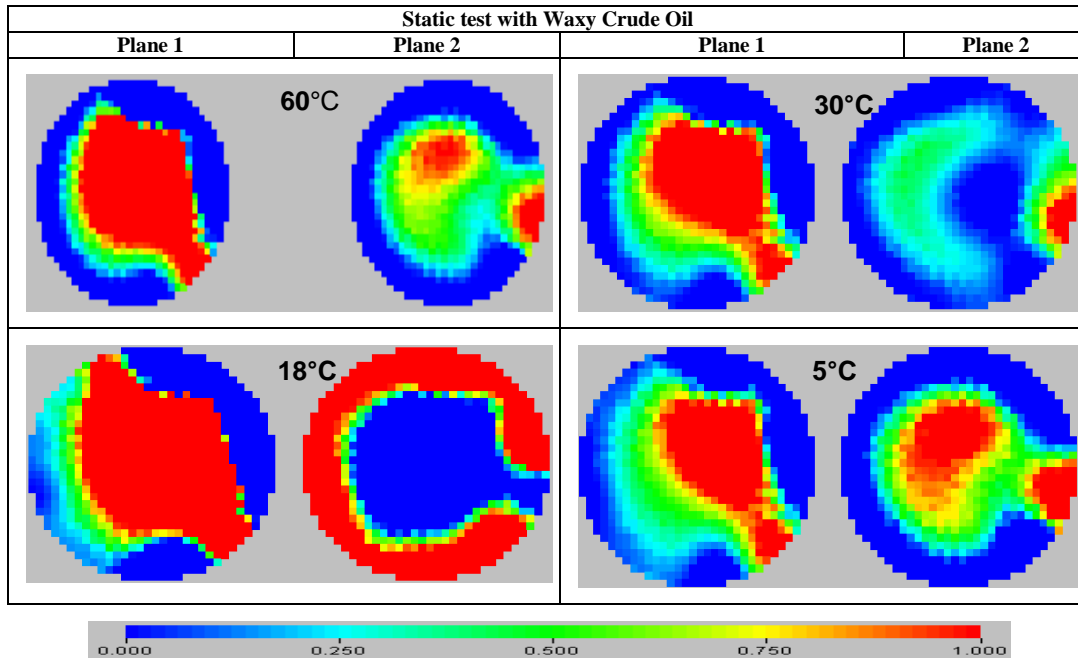


Figure 8 Tomogram images for Planes 1 and 2

3.3 Estimation of Void Fraction using Normalised Capacitance and Pixel

3.3.1 Effect of Temperature on Normalised Capacitance

Figure 9 shows the graph between the temperature and normalised capacitance of Plane 1 for the electrode pair 1-3 (i.e., 1-adjacent), 1-5 (i.e., 3-adjacent), and 1-7 (i.e., opposite). It shows that as the temperature keeps increasing for electrode pair 1-3, the raw capacitance is increasing. But for electrode pairs 1-5 and 1-7 the behavior of capacitance is different; an increase in temperature after 35°C caused the normalised capacitance to slightly decrease. The value for Plane 1 lies in $0.07 \geq C_n \geq 0.23$ that is within the permissible range of 0 to 1. It also follows a linear relation between temperature and capacitance.

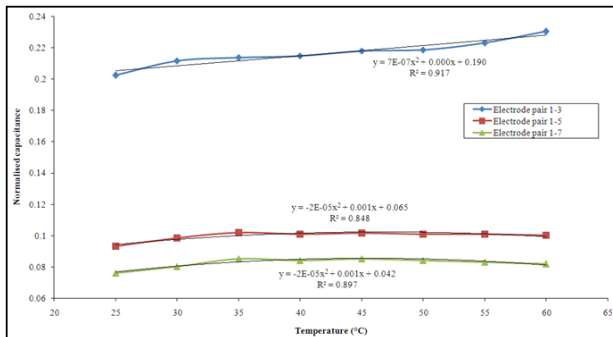


Figure 9 Temperature versus normalised capacitance for Plane 1

Figure 10 shows the graph between the temperature and normalised capacitance of Plane 2 for the electrode pair 1-3 (i.e., 1-adjacent), 1-5 (i.e., 3-adjacent), and 1-7 (i.e., opposite). The change in normalised capacitance for Plane 1 and Plane 2 is increasing on an increase in temperature. But the behavior of electrode pairs 1-5 and 1-7 for both planes is different; for electrode pair 1-5 in plane 2, the normalised capacitance is

decreasing on increase in temperature and for electrode pair 1-7 the normalised capacitance is increasing. The range of C_n for Plane 2 is from $0.01 \geq C_n \geq 0.23$ i.e. also within the acceptable range. The difference in trend of electrode pair 1-5 and 1-7 between Plane 1 and Plane 2 could be because of the external interference such as; signal-to-noise ratio or error in the electrode geometry.

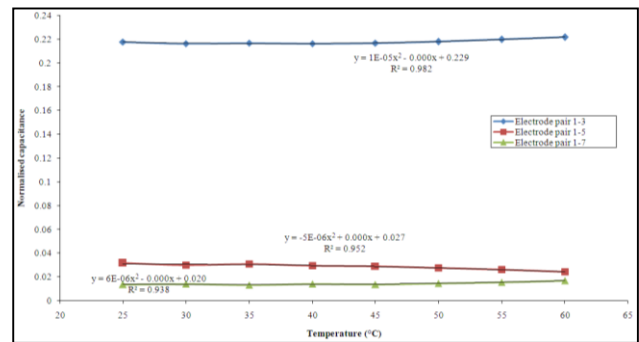


Figure 10 Temperature versus normalised capacitance for Plane 2

3.3.2 Void Fraction Calculation Using Normalised Capacitance

The average voidage can be calculated by summing all the normalised capacitance values for one image frame dividing by the sum of the normalised capacitances when the sensor filled with higher permittivity material. By using equation (3), the volume ratio is calculated at different temperature of waxy crude oil using Parallel ECT model. Figure 11 shows the graph plotted between temperature and the voidage calculation in % for Plane 1 and Plane 2. The trend of plot for both the planes is symmetrical. The range of voidage values based on the normalised inter-electrode capacitance measurements is from 0.995 to 0.999 i.e. less than a permissible range of 0 to 1.

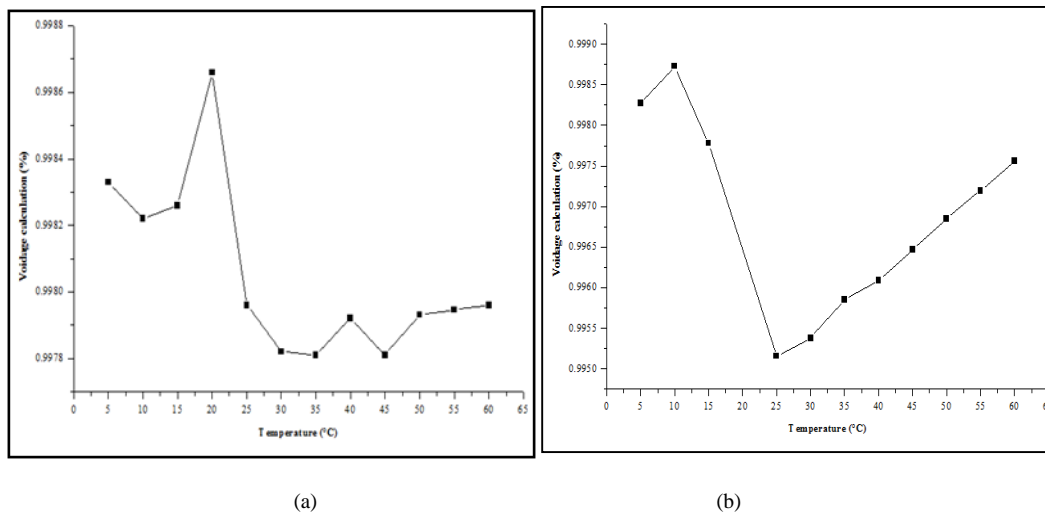


Figure 11 Temperature *versus* void fraction based on normalised capacitance: (a) Plane 1, and (b) Plane 2

3.3.3 Effect of Temperature on Normalised Pixel Based Void

Figure 12 shows the preliminary result for void fraction obtained from image pixels based on the change in temperature. The range it covers lies in between $0.06 \geq \alpha \geq 0.04$. From the graph it can be observed that void fraction is linearly decreasing from 65°C till 25°C, however, from 20°C till 5°C it shows an abrupt behavior. On comparison between the results of void fraction obtained from normalised capacitance or normalised pixels, the trend of graph is similar.

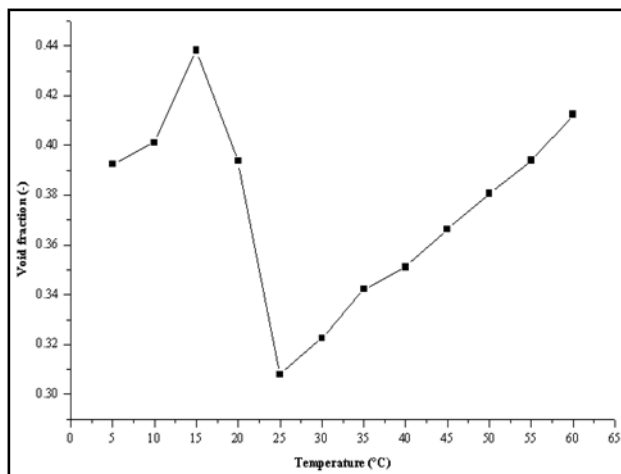


Figure 12 Temperature *versus* void fraction based on normalised pixel

4.0 CONCLUSIONS

A dual-plane ECT sensor (12 electrodes per plane) has been designed and fabricated successfully for the measurement of thermal shrinkage and gas void formation in waxy cooled crude oil. During the experiment some interesting behaviors of waxy crude oil has been observed. Calibration of dual plane sensor has been done using air and deionised water as low and high permittivity material. It has been used to determine the raw capacitance and analyzes the behavior of waxy crude at the

change of temperature by using the tomogram images. A correlation between two planes still needs to be developed in subsequent stage and to determine the void formation based on temperature change. Pixel data obtained from ECT also used to calculate the initial values of waxy cooled crude oil void fraction based on varying the temperature.

The main significance of this research is the application of non-invasive/non-intrusive techniques i.e. ECT for the measurement of thermal shrinkage and gas voids formation in waxy crude oil in subsea pipelines. It analyzes the formation of the gelled crude characteristics under different cooling scenarios. The experimental data of this research work could be used as a basis in order to determine the nature of the gelled crude and its compressibility for the accurate prediction of restart pressure. It can also be helpful to understand the phenomenon of void fraction in waxy crude based on varying the temperature and pressure. The prediction of waxy crude oil behavior also provides accuracy in designing and planning of sub-sea pipelines.

Acknowledgement

The authors would like to thank Universiti Teknologi PETRONAS (UTP) for sponsoring the research and providing test facilities.

References

- [1] I. Frigaard, Vinay, G. and Wachs, A. 2007. Compressible Displacement of Waxy Crude Oils in Long Pipeline Startup Flows. *Journal of Non-Newtonian Fluid Mechanics*. 147: 45–64.
- [2] K. Karan, Ratulowski, J. and German, P. 2000. Measurement of Waxy Crude Properties Using Novel Laboratory Techniques. Presented at the SPE Annual Technical Conference and Exhibition, Dallas, Texas.
- [3] G. Vinay, Wachs, A. and Agassant, J. F. 2005. Numerical Simulation of Non-isothermal Viscoplastic Waxy Crude Oil Flows. *Journal of Non-Newtonian Fluid Mechanics*. 128: 144–162.
- [4] R. a. A. Hoffmann, L. 2010. Single-Phase Wax Deposition Experiments. *Energy Fuels*. 24: 1069–1080.
- [5] J. F. Tinsley, Jahnke, J. P., Adamson, D. H., Guo, X., Amin, D., Kriegel, R., Saini, R., Dettman, H. D. and Prud'home, R. K., 2009.

- Waxy Gels with Asphaltenes 2: Use of Wax Control Polymers. *Energy & Fuels*. 23: 2065–2074.
- [6] C. K. Ewkeribe, 2008. Quiescent Gelation of Waxy Crudes and Restart of Shut-in Subsea Pipelines. MASTER OF SCIENCE, UNIVERSITY OF OKLAHOMA GRADUATE COLLEGE, Norman, Oklahoma.
- [7] H. Alboudwarej, Huo, Z. and Kempton, E. 2006. Flow-Assurance Aspects of Subsea Systems Design for Production of Waxy Crude Oils. Presented at the SPE Annual Technical Conference and Exhibition., San Antonio, Texas, USA.
- [8] T. T. Ruiz. 2010. Experimental Investigation of Restarting Fully-gelled Subsea Waxy-oil Pipelines. MASTER OF SCIENCE, University of Oklahoma, Norman, Oklahoma.
- [9] C. Ekweribe, Civan, F., Lee, H.S. and Singh, P. 2009. Interim Report on Pressure Effect on Waxy-Crude Pipeline-Restart Conditions Investigated by a Model System. *SPE Projects, Facilities & Construction*. 4: 612009.74. September 2009.
- [10] D. A. Phillips, Forsdyke, I. N., McCracken, I. R. and Ravenscroft, P. D. 2011. Novel Approaches to Waxy Crude Restart: Part 1: Thermal Shrinkage of Waxy Crude Oil and the Impact for Pipeline Restart. *Journal of Petroleum Science and Engineering*. 77: 237–253.
- [11] M. Margarone, Borghi, G. and Corra, S. 2010. One dimensional Modelling and Experimental Validation Of Gelled Waxy Oil Restart. Presented at the North Africa Technical Conference and Exhibition, Cairo, Egypt.
- [12] G. Vinay, Wachs, A. and Frigaard, I. 2007. Start-up Transients and Efficient Computation of Isothermal Waxy Crude Oil Flows. *Journal of Non-Newtonian Fluid Mechanics*. 143: 141–156.
- [13] I. Hénaut, Vincké, O. and Brucy, F. 1999. Waxy Crude Oil Restart: Mechanical Properties of Gelled Oils. Presented at the SPE Annual Technical Conference and Exhibition, Houston, Texas.
- [14] C. Chang, Boger, D. V. and Nguyen, Q. D. 1998. The Yielding of Waxy Crude Oils. *Ind. Eng. Chem. Res.* 37: 1551–1559.
- [15] A. Hunt, J. Pendleton, and Y. Ladam. 2004. Visualisation of two-Phase Gas-liquid Pipe Flows Using Electrical Capacitance Tomography. In *7th Biennial ASME Conference on Engineering Systems Design and Analysis*, Manchester, UK. 5.
- [16] K. J. a. M. Alme, S. 2006. Electrical Capacitance Tomography; Sensor Models, Design, Simulations, and Experimental Verification. *Sensors Journal, IEEE*. 6: 1256–1266.
- [17] S. S. Donthi. 2004. Capacitance based Tomography for Industrial Applications. EE Dept. IIT, Bombay.
- [18] W. Q. Yang. 2010. Design of Electrical Capacitance Tomography Sensors. *Measurement Science and Technology*. 21, 18 February 2010.
- [19] W. Q. Yang, A. Chondronasios, S. Nattrass, V. T. Nguyen, M. Betting, I. Ismail, *et al.* 2004. Adaptive Calibration of a Capacitance Tomography System for Imaging Water Droplet Distribution. *Flow Measurement and Instrumentation*. 15: 249–258.
- [20] I. a. Y. Ismail, W. Q. 2005. Application of Electrical Capacitance Tomography in Wet Gas Flow Metering. Presented at the 4th International South East Asia Hydrocarbon Flow Measurement Workshop.
- [21] Z. Huang, Wang, B. and Li, H., 2003. Application of Electrical Capacitance Tomography to the Void Fraction Measurement of Two-Phase Flow. *Instrumentation and Measurement, IEEE Transactions on*. 52: 7–12.